EDGE ARTICLE

Check for updates

Photocatalytic oxidation of benzene to phenol using dioxygen as an oxygen source and water as an electron source in the presence of a cobalt catalyst†

Ji Won Han,‡[a] Jieun Jung,‡[ab] Yong-Min Lee, [iD][a] Wonwoo Nam [iD]*[a] and Shunichi Fukuzumi [iD]*[ac]

Photocatalytic hydroxylation of benzene to phenol by dioxygen (O_2) occurs under visible light irradiation of an O_2-saturated acetonitrile solution containing $[Ru^{II}(Me_2phen)_3]^{2+}$ as a photocatalyst, $[Co^{III}(Cp^*)(bpy)(H_2O)]^{2+}$ as an efficient catalyst for both the water oxidation and benzene hydroxylation reactions, and water as an electron source in the presence of $Sc(NO_3)_3$. The present study reports the first example of photocatalytic hydroxylation of benzene with O_2 and H_2O, both of which are the most green reagents, under visible light irradiation to afford a high turnover number (*e.g.*, >500). Mechanistic studies revealed that the photocatalytic reduction of O_2 to H_2O_2 is the rate-determining step, followed by efficient catalytic hydroxylation of benzene to phenol with H_2O_2, paving a new way for the photocatalytic oxygenation of substrates by O_2 and water.

Introduction

Phenol, which is an important precursor for many chemicals and industrial products (*e.g.*, dyes, polymers, *etc.*), is currently produced from benzene by a three step cumene process.[1,2] Since the efficiency of the cumene process is low (~5% yield of phenol) under severe conditions (*e.g.*, high temperature, high pressure, and strong acidic conditions), it is highly desired to develop a one-step synthesis of phenol from benzene using homogeneous and heterogeneous inorganic catalysts.[3–5] Among various oxidants, hydrogen peroxide (H_2O_2) is frequently used as a green oxidant, which produces water or dioxygen (O_2) as products, in catalytic benzene hydroxylation.[6–13] O_2 is a more ideal oxidant than H_2O_2 because of its abundance in nature, low cost, and environmental benignity.[4,14,15] However, catalytic aerobic oxidation of benzene to phenol has required sacrificial reducing agents such as H_2, ascorbic acid, and NADH analogs.[16] In addition, the catalytic aerobic oxidation of benzene without sacrificial reducing agents has so far required harsh conditions, such as high temperatures or UV light photoirradiation.[14,15,17,18] Moreover,

although the photocatalytic hydroxylation of benzene to phenol using organic photocatalysts without overoxidation has been demonstrated,[19–22] the turnover numbers (TONs) of the catalytic hydroxylation of benzene to phenol are still low (*e.g.*, 13).[20]

We report herein an efficient photocatalytic hydroxylation of benzene to phenol (PhOH) using O_2 as an oxidant in the presence of $Sc(NO_3)_3$ and utilizing $[Ru^{II}(Me_2phen)_3]^{2+}$ ($Me_2phen = $ 4,7-dimethyl-1,10-phenanthroline) as a photocatalyst, water as an electron source, and $[Co^{III}(Cp^*)(bpy)(H_2O)]^{2+}$ ($Cp^* = \eta^5$-pentamethylcyclopentadienyl and bpy = 2,2-bipyridine) as an efficient catalyst for water oxidation as well as benzene hydroxylation to attain a TON of greater than 500 (Scheme 1). Mechanistic aspects of the benzene hydroxylation reaction under the visible light irradiation conditions have been discussed as well.

Results and discussion

$[Co^{III}(Cp^*)(bpy)(H_2O)]^{2+}$ (**1**) and $[Ru^{II}(Me_2phen)_3]^{2+}$ were synthesised according to the literature methods.[23,24] Visible light irradiation of an O_2-saturated solution of CH_3CN (MeCN) and H_2O (v/v = 23 : 2) containing a catalytic amount of **1** (1.0 μM), $[Ru^{II}(Me_2phen)_3]^{2+}$ (1.0 mM), $Sc(NO_3)_3$ (100 mM), and benzene (1.0 M) at 298 K resulted in the formation of PhOH [eqn (1)],

$$PhH + \frac{1}{2}O_2 \xrightarrow[\text{cat.}]{h\nu} PhOH \tag{1}$$

as shown in Fig. 1. PhOH is produced *via* the catalytic oxygenation of hydrogen peroxide (H_2O_2) with **1**, which acts as not only a benzene oxygenation catalyst but also a water oxidation catalyst

[a]*Department of Chemistry and Nano Science, Ewha Womans University, Seoul 03760, Korea. E-mail: fukuzumi@chem.eng.osaka-u.ac.jp; wwnam@ewha.ac.kr*

[b]*Department of Chemistry, Graduate School of Science, Nagoya University, Chikusa, Nagoya 464-8602, Japan*

[c]*Faculty of Science and Engineering, Meijo University, SENTAN, Japan Science and Technology Agency (JST), Nagoya, Aichi 468-8502, Japan*

† Electronic supplementary information (ESI) available: Table S1 and Fig. S1–S8. See DOI: 10.1039/c7sc02495a

‡ These authors contributed equally to this work.

Scheme 1 Mechanism of the photocatalytic hydroxylation of benzene.

Fig. 1 Time courses of the products [PhOH (blue) and *p*-benzoquinone (red)] obtained in the photocatalytic oxidation of benzene by O_2 with $[Ru^{II}(Me_2phen)_3]^{2+}$ (1.0 mM) in the presence of a catalytic amount of **1** (1.0 μM) in an O_2-saturated solvent mixture of MeCN and H_2O (v/v = 23 : 2) containing $Sc(NO_3)_3$ (100 mM) and benzene (1.0 M) under photoirradiation (white light) at 298 K.

with $[Ru^{III}(Me_2phen)_3]^{3+}$ produced by photoinduced electron transfer from the excited state of $[Ru^{II}(Me_2phen)_3]^{2+}$ to O_2 in the presence of Sc^{3+}, as shown in Scheme 1. It should be noted that the catalyst **1** acts as an efficient catalyst for water oxidation in the photocatalytic production of H_2O_2 in the presence of $Sc(NO_3)_3$, as reported previously.[23,25] $[Ru^{II}(Me_2phen)_3]^{2+}$ acts as a more efficient photocatalyst compared to $[Ru^{II}(bpy)_3]^{2+}$ for O_2 reduction by the excited state, because the one-electron oxidation potential of $[Ru^{II}(Me_2phen)_3]^{2+*}$ ($E_{ox}^* = -1.01$ V *vs.* NHE) is more negative than that of $[Ru^{II}(bpy)_3]^{2+*}$ ($E_{ox}^* = -0.84$ V *vs.*

NHE).[23] The UV-vis spectrum of the photocatalyst, $[Ru^{II}(Me_2phen)_3]^{2+}$, during the photocatalytic oxidation remained almost identical to that of the initial stage at 445 nm, indicating that the overall reactivity decreased with time due to oxidative degradation of the catalyst **1** (see Experimental section; Fig. S1, ESI†).

p-Benzoquinone was also produced during the photocatalytic oxidation of benzene by O_2, and the yield of *p*-benzoquinone increased as the reaction solution was irradiated for a longer time but the yield of PhOH remained constant (Fig. 1). The observation of the induction period for the formation of *p*-benzoquinone in Fig. 1 suggests that *p*-benzoquinone is produced by the further oxidation of PhOH. The production of *p*-benzoquinone from PhOH was independently confirmed (Fig. S2, ESI†). The TON for the production of both phenol and benzoquinone based on **1** was determined to be 500(20), where the TON of *p*-benzoquinone is counted three times because *p*-benzoquinone is the six-electron oxidized product whereas phenol is the two-electron oxidized product. When the reaction conditions were changed by increasing the concentration of the catalyst and decreasing the concentration of the benzene substrate, a much higher product yield of phenol (~30%) based on benzene was obtained (Fig. 2) than that in Fig. 1. The quantum yield (QY) was estimated by eqn (2),

$$QY\ (\%) = R/I \times 100 \qquad (2)$$

where R (mol s^{-1}) is the PhOH production rate and I (einstein s^{-1}) is the rate of the number of incident photons. The quantum yield was determined to be 1.7(2)% from the amount of PhOH produced during the photocatalytic reaction under photoirradiation ($\lambda = 440$ nm) for 1 h (Fig. S3, ESI†). The photocatalytic reactivity increased on increasing the concentration of benzene as well as the concentration of $[Ru^{II}(Me_2phen)_3]^{2+}$ (Fig. S4, ESI†). A negligible amount of PhOH was produced in the absence of **1**, indicating that **1** is an essential component in the benzene hydroxylation reaction.

Fig. 2 Time courses of PhOH concentration produced in the photocatalytic oxidation of benzene under photoirradiation (white light) of an O_2-saturated solvent mixture of MeCN and H_2O (v/v = 23 : 2) containing **1** (0.10 mM), $[Ru^{II}(Me_2phen)_3]^{2+}$ (1.0 mM), and benzene (1.0 mM, blue circles) or benzene-d_6 (1.0 mM, red circles) in the presence of $Sc(NO_3)_3$ (100 mM) at 298 K. No *p*-benzoquinone was produced under the present experimental conditions.

The photocatalytic hydroxylation reaction proceeds as shown in Scheme 1. Visible light irradiation of $[Ru^{II}(Me_2phen)_3]^{2+}$ resulted in the formation of H_2O_2 by oxidative quenching of the photoexcited state $[Ru^{II}(Me_2phen)_3]^{2+*}$ (* denotes the excited state) with O_2 in the presence of $Sc(NO_3)_3$ (Scheme 1, reaction pathways b and c), as reported for the case of $[Ru^{II}(bpy)_3]^{2+}$.[26] The time courses of $[Ru^{III}(Me_2phen)_3]^{3+}$ generation and H_2O_2 production were obtained to give the stoichiometry of the photochemical reaction, as shown in eqn (3) (Fig. 3).

$$2[Ru^{II}(Me_2phen)_3]^{2+} + O_2 + 2H^+ \xrightarrow{h\nu} 2[Ru^{III}(Me_2phen)_3]^{3+} + H_2O_2 \quad (3)$$

The lifetime of $[Ru^{II}(Me_2phen)_3]^{2+*}$ and emission quenching have been determined to obtain the rate constants (k_{et}) of photoinduced electron transfer in the absence and presence of $Sc(NO_3)_3$ (Fig. S5 and Table S1, ESI†). The k_{et} values in both the absence and presence of $Sc(NO_3)_3$ are close to the diffusion-limited value, showing that $Sc(NO_3)_3$ does not affect the oxidative quenching of $[Ru^{II}(Me_2phen)_3]^{2+*}$ by O_2. The emission spectra of $[Ru^{II}(Me_2phen)_3]^{2+}$ in the absence and presence of $Sc(NO_3)_3$ taken in a solvent mixture of MeCN and H_2O (v/v = 23 : 2) containing different concentrations of O_2 indicate that the amount of O_2 in air is large enough for efficient H_2O_2 photogeneration (Fig. S5d, ESI†).

Visible light irradiation of the reaction solution without benzene results in the formation of H_2O_2, as shown in Fig. 4 (Scheme 1, reaction pathways a–c), and the production of H_2O_2 is obtained from the photooxidation of $[Ru^{II}(Me_2phen)_3]^{2+}$ by O_2 [eqn (3)] and the catalytic water oxidation by $[Ru^{III}(Me_2phen)_3]^{3+}$ in the presence of **1** [eqn (4)].[23] Thus, the overall reaction

$$2[Ru^{III}(Me_2phen)_3]^{3+} + H_2O \xrightarrow{cat.} 2[Ru^{II}(Me_2phen)_3]^{2+} + \frac{1}{2}O_2 + 2H^+ \quad (4)$$

is the photocatalytic oxidation of H_2O by O_2 to produce H_2O_2, as given by eqn (5).

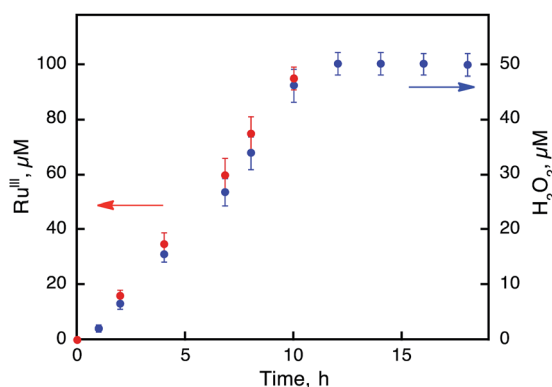

Fig. 3 Time courses of the concentrations of $[Ru^{III}(Me_2phen)_3]^{3+}$ (red) and H_2O_2 (blue) produced from H_2O and O_2 in the photocatalytic oxidation of $[Ru^{II}(Me_2phen)_3]^{2+}$ by O_2 under photoirradiation (white light) of an air-saturated solvent mixture of MeCN and H_2O (v/v = 23 : 2) containing $[Ru^{II}(Me_2phen)_3]^{2+}$ (100 μM) in the presence of $Sc(NO_3)_3$ (100 mM) at 298 K.


Fig. 4 Time courses of the photocatalytic production of H_2O_2 from H_2O and O_2 with $[Ru^{II}(Me_2phen)_3]^{2+}$ (0.10 mM) in the presence of a catalytic amount of **1** [0.50 mM (red), 1.0 mM (orange), 1.5 mM (green), and 2.0 mM (blue)] in an air-saturated solvent mixture of MeCN and H_2O (v/v = 23 : 2) containing $Sc(NO_3)_3$ (100 mM) under photoirradiation (white light) at 298 K.

$$H_2O + \frac{1}{2}O_2 \xrightarrow[cat.]{h\nu} H_2O_2 \quad (5)$$

The rates of photocatalytic oxidation of H_2O by O_2 to produce H_2O_2 in the presence of **1** were also investigated with various concentrations of **1** at 298 K (Fig. S6, ESI†). The zeroth-order rate constants (k_{obs}) were obtained from the initial slopes of the plots of the amount of H_2O_2 produced vs. time, being proportional to the concentration of **1** (Fig. 4 and S6, ESI†).

The catalytic water oxidation by $[Ru^{III}(Me_2phen)_3]^{3+}$ with **1** to evolve O_2 [eqn (6); Scheme 1, reaction pathway a]

$$2H_2O + 4Ru^{III} \xrightarrow{cat.} O_2 + 4H^+ + 4Ru^{II} \quad (6)$$
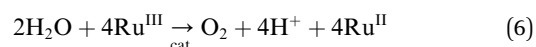
was independently confirmed, where O_2 was evolved, accompanied by the formation of $[Ru^{II}(Me_2phen)_3]^{2+}$. The evolved O_2 concentrations were investigated by a Clark oxygen electrode, showing an increase in the amount of O_2 evolved after addition of $[Ru^{III}(Me_2phen)_3]^{3+}$ (1.0 mM) to a solvent mixture of MeCN and H_2O (1.0 mL; v/v = 9 : 1) containing $Sc(NO_3)_3$ (100 mM) and various concentrations of **1** (Fig. 5), where the O_2 yield increased with an increasing concentration of **1** to approach 100% (1/4 of the initial concentration of $[Ru^{III}(Me_2phen)_3]^{3+}$). The reaction rate was accelerated with an increasing concentration of **1** to account for oxidation of water by $[Ru^{III}(Me_2phen)_3]^{3+}$ with **1** under acidic conditions due to the presence of $Sc(NO_3)_3$. Formation of $[Ru^{II}(Me_2phen)_3]^{2+}$ accompanied by water oxidation was also confirmed by monitoring the UV-vis spectral changes (Fig. S7a, ESI†). The time courses of the oxidation of **1** by $[Ru^{III}(Me_2phen)_3]^{3+}$ were obtained by spectral changes at $\lambda = 445$ nm due to $[Ru^{II}(Me_2phen)_3]^{2+}$, showing that the rate of $[Ru^{II}(Me_2phen)_3]^{2+}$ formation from $[Ru^{III}(Me_2phen)_3]^{3+}$ increased with the increase of the concentration of **1** (Fig. S7b, ESI†).

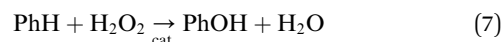Catalytic oxidation of benzene to phenol with H_2O_2 [eqn (7)]

$$PhH + H_2O_2 \xrightarrow{cat.} PhOH + H_2O \quad (7)$$

Fig. 5 Time courses of O_2-evolution observed in the catalytic oxidation of H_2O by $[Ru^{III}(Me_2phen)_3]^{3+}$ (1.0 mM) with **1** [10 μM (red), 50 μM (orange), 100 μM (green), and 200 μM (blue)] in the presence of $Sc(NO_3)_3$ (100 mM) in a deaerated solvent mixture (1.0 mL) of MeCN and H_2O (v/v = 9 : 1) at 298 K. The induction periods were observed due to the reaction time to oxidize **1** by $[Ru^{III}(Me_2phen)_3]^{3+}$ to produce the catalytically active species.

has also been confirmed in a solvent mixture of MeCN and H_2O (23 : 2) containing $Sc(NO_3)_3$ in order to stabilize H_2O_2 with the same conditions for the overall photocatalytic reaction as shown in Fig. 6 (Scheme 1, reaction pathway d). The rate of benzene hydroxylation increased with increasing concentrations of **1** (Fig. 6) and H_2O_2 (Fig. S8, ESI†). A combination of the photocatalytic oxidation of H_2O by O_2 to produce H_2O_2 [eqn (5)] and the catalytic hydroxylation of benzene to phenol by H_2O_2 [eqn (7)] affords the overall photocatalytic oxidation of benzene to phenol by O_2 [eqn (1)]. The photocatalytic reactions of an O_2-saturated solution of MeCN and H_2O (v/v = 23 : 2) containing **1** (0.50 mM), $[Ru^{II}(Me_2phen)_3]^{2+}$ (0.10 mM), and $Sc(NO_3)_3$ (100 mM) under photoirradiation (white light) were examined in the absence and presence of benzene to compare their reactivities (Fig. 7). The rate of H_2O_2 production from H_2O and O_2 in the absence of benzene was slightly higher than that of PhOH generation in the photocatalytic hydroxylation of benzene, indicating that H_2O_2 produced in the photocatalytic oxidation

of H_2O by O_2 reacted with benzene efficiently in the presence of **1** to produce PhOH.[27] In fact, the rate of PhOH production (59 μM after 1 h) from H_2O_2 (1.0 mM) and benzene (1.0 M) with **1** (0.50 mM, red dots in Fig. 6) is much faster than that of PhOH production (estimated to be 7.5 μM after 1 h) in the photocatalytic reaction (Fig. 7), because the concentration of H_2O_2 produced in the photocatalytic oxidation of H_2O by O_2 is much smaller than 1.0 mM. Since the rate of PhOH production from H_2O_2 is proportional to the concentration of H_2O_2 (Fig. S8, ESI†), the rate of PhOH production in the photocatalytic hydroxylation of benzene by O_2 corresponds to that of PhOH production in the catalytic oxidation of benzene with 127 μM H_2O_2, which may be the steady state concentration during the photocatalytic hydroxylation of benzene.

Then, $^{18}O_2$-labeling experiments were performed to confirm that the oxygen atom in the phenol product in eqn (1) derives from O_2 (Fig. 8). Indeed, $Ph^{18}OH$ (73%) was formed as the major product together with $Ph^{16}OH$ (27%) in the $^{18}O_2$-labeling experiments, indicating that the oxygen atom in the PhOH product obtained in the photocatalytic oxidation of benzene by $H_2^{18}O_2$ derived from $^{18}O_2$ (98% ^{18}O-enriched; Fig. 8). The formation of $Ph^{16}OH$ (27%) indicates that $^{16}O_2$ was produced by the oxidation of $H_2^{16}O$ by $[Ru^{III}(Me_2phen)_3]^{3+}$, leading to the production of $H_2^{16}O_2$ to oxidize benzene to produce $Ph^{16}OH$ instead of $Ph^{18}OH$ (Scheme 1, reaction pathway a). The ^{18}O-labeling experiments were also performed by replacing $H_2^{16}O$ with $H_2^{18}O$ to support that the oxygen atom in the phenol product derives from O_2 rather than H_2O (Fig. 9). In this case, $Ph^{16}OH$ (66%) was the major product together with $Ph^{18}OH$ (34%), consistent with the $^{18}O_2$-labeling experiments described above.

The photocatalytic mechanism of benzene hydroxylation to phenol by O_2 is summarized in Scheme 1. The photoexcitation of $[Ru^{II}(Me_2phen)_3]^{2+}$ in an O_2-saturated solvent mixture of MeCN and H_2O (v/v = 23 : 2) containing $Sc(NO_3)_3$ resulted in electron transfer from the triplet excited state of $[Ru^{II}(Me_2phen)_3]^{2+}$ to O_2 to produce $[Ru^{III}(Me_2phen)_3]^{3+}$ and the $O_2^{\bullet-}$–Sc^{3+} complex.[23,28] The strong binding of Sc^{3+} to $O_2^{\bullet-}$, which was

Fig. 6 Time courses of the catalytic hydroxylation of benzene to PhOH with H_2O_2 (1.0 mM) in the presence of **1** [10 μM (black), 50 μM (blue), 100 μM (green), and 500 μM (red)] in a solvent mixture of MeCN and H_2O (v/v = 23 : 2) containing benzene (1.0 M) and $Sc(NO_3)_3$ (100 mM) at 298 K.

Fig. 7 Time courses of the products from the photoinduced reaction under photoirradiation (white light) in an O_2-saturated solvent mixture of MeCN and H_2O (v/v = 23 : 2) containing **1** (0.50 mM), $[Ru^{II}(Me_2phen)_3]^{2+}$ (0.10 mM), and $Sc(NO_3)_3$ (100 mM) in the absence (blue) and presence (red) of benzene (1.0 M) at 298 K.

Fig. 8 A comparison of the relative abundances of authentic PhOH (blue) and the PhOH product (red) yielded in the photocatalytic hydroxylation of benzene by **1** (0.10 mM) in the presence of $[Ru^{II}(Me_2phen)_3]^{2+}$ (1.0 mM), $Sc(NO_3)_3$ (100 mM), and benzene (2.0 M) under photoirradiation (white light) in an $^{18}O_2$-saturated solvent mixture of MeCN and H_2O (v/v = 23 : 2) at 298 K for 24 h. The peaks at m/z = 94 and 96 correspond to $Ph^{16}OH$ and $Ph^{18}OH$, respectively.

Fig. 9 A comparison of the relative abundances of authentic PhOH (blue) and the produced PhOH (red) in the photocatalytic hydroxylation of benzene by O_2 with **1** (0.10 mM) in the presence of $[Ru^{II}(Me_2phen)_3]^{2+}$ (1.0 mM), $Sc(NO_3)_3$ (100 mM), and benzene (2.0 M) under photoirradiation (white light) of an $^{16}O_2$-saturated solvent mixture of MeCN and $H_2^{18}O$ (v/v = 23 : 2) at 298 K for 24 h. The peaks at m/z = 94 and 96 correspond to $Ph^{16}OH$ and $Ph^{18}OH$, respectively.

detected by EPR, inhibits the back electron transfer from the $O_2^{\cdot-}$–Sc^{3+} complex to $[Ru^{III}(Me_2phen)_3]^{3+}$, followed by disproportion with H_2O to produce H_2O_2.[23] H_2O_2 has attracted considerable attention as an ideal solar fuel for a one-compartment H_2O_2 fuel cell with a theoretical maximum output potential of 1.09 V, which is comparable to that of a hydrogen fuel cell (1.23 V).[23] $[Ru^{III}(Me_2phen)_3]^{3+}$ can oxidize H_2O to O_2 with catalysis by **1**. Benzene hydroxylation to PhOH was also catalysed by **1**. As reported previously, the NMR peaks assignable to the bpy and Cp* of **1** remained the same after the photocatalytic production of H_2O_2, indicating that **1** acted as a homogeneous catalyst during the reaction.[23] However, the catalytically active intermediates such as the Co(IV)-oxo species[29] have yet to be detected in the catalytic benzene hydroxylation with H_2O_2. There was no deuterium kinetic isotope effect (KIE) for benzene (Fig. 2), indicating that C–H bond cleavage is not involved in the rate-determining step of the photocatalytic hydroxylation reaction.

Conclusions

In conclusion, we have shown that benzene is oxidized to phenol by dioxygen with a high TON (*e.g.*, 500) under visible light irradiation of a reaction solution containing $[Ru^{II}(Me_2phen)_3]^{2+}$ as a photocatalyst, $[Co^{III}(Cp*)(bpy)(H_2O)]^{2+}$ as an efficient catalyst for both water oxidation and benzene hydroxylation, and water as an electron source in the presence of $Sc(NO_3)_3$. The combination of the photocatalytic H_2O_2 production by H_2O oxidation with O_2 and the catalytic hydroxylation of benzene to phenol with H_2O_2 demonstrated in this study has paved a new road towards direct oxygenation of substrates by O_2 as the most environmentally benign oxidant as well as oxygen source without any electron source except H_2O, which is also the most environmentally benign hydrogen source.

Experimental section

Materials

All solvents and chemicals were of reagent-grade quality, obtained commercially and used without further purification, unless otherwise noted. Ruthenium(III) chloride hydrate, ammonium hexafluorophosphate, *n*-butyllithium solution (2.7 M in heptane), *n*-pentane, and tetrahydrofuran were purchased from Aldrich Chemicals. The chemicals, such as 4,7-dimethyl-1,10-phenanthroline (Me_2phen), silver sulphate, lead dioxide, and cobalt(II) chloride, were purchased from Alfa Aesar. 2,2′-Bipyridine, 1,2,3,4,5-pentamethylcyclopentadiene, and $Ti^{IV}(O)(tpyp)$ (tpyp = 5,10,15,20-tetra(4-pyridyl)porphyrinato anion) were obtained from Tokyo Chemical Industry Co., Ltd. $Sc(NO_3)_3·4H_2O$ was supplied by Mitsuwa Chemicals Co., Ltd. $^{18}O_2$ gas (98% ^{18}O-enriched) was purchased from ICON Services Inc. (Summit, NJ. USA). The purification of water (18.2 MΩ cm) was performed with a Milli-Q system (Millipore, Direct-Q 3 UV). Acetonitrile was dried according to published procedures and distilled prior to use.[30] The cobalt(III) starting complex, $[Co^{III}(Cp*)(bpy)(H_2O)]^{2+}$ (**1**, Cp* = η^5-pentamethylcyclopentadienyl and bpy = 2,2-bipyridine), and the tris(4,7-dimethyl-1,10-phenanthroline)ruthenium(II) complex, $[Ru^{II}(Me_2phen)_3]^{2+}$, were prepared according to the published methods.[25,31]

Instrumentation

UV-vis spectra were recorded on a Hewlett Packard 8453 diode array spectrophotometer equipped with a UNISOKU Scientific Instruments Cryostat USP-203A. Product analysis for the oxidation reactions was performed with an Agilent Technologies 6890N gas chromatograph (GC) and a Thermo Finnigan (Austin, Texas, U.S.A.) FOCUS DSQ (dual stage quadrupole) mass spectrometer interfaced with a Finnigan FOCUS gas chromatograph (GC-MS). The amount of evolved oxygen was recorded by a Clark-type oxygen electrode made by Hansatech Ltd.

Product analysis

The products formed in the oxidation of benzene by **1** and O_2 in the presence of $[Ru^{II}(Me_2phen)_3]^{2+}$ and $Sc(NO_3)_3$ in a solvent mixture of MeCN and H_2O (v/v = 23 : 2) at 298 K were identified by GC and GC-MS by a comparison of the mass peaks and retention time of the products with respect to the authentic samples, and the product yields were determined by comparing the responsive peak areas of the sample products against standard curves prepared with known authentic compounds using the internal standard decane. The quantum yield (QY) of the photocatalytic hydroxylation of benzene has been determined under visible light irradiation of mono-chromatized light using a Compact Xenon Light Source (MAX-302; Asahi Spectra Co., Ltd). The amount of hydrogen peroxide produced was determined by spectroscopic titration with an acidic solution of a $[Ti^{IV}O(tpypH_4)]^{4+}$ complex.[31] $[Ti^{IV}O(tpypH_4)]^{4+}$ (50 µM) was prepared by dissolving 3.4 mg of the TiO(tpyp) complex into water (100 mL) containing hydrochloric acid (50 mM). A small portion (100 µL) of the photocatalytic reaction solution was taken and diluted up to 1.0 mL with water. To 0.25 mL of the diluted sample, 0.25 mL of perchloric acid (4.8 M) and 0.25 mL of $[Ti^{IV}O(tpypH_4)]^{4+}$ (50 µM) were added. The mixed solution was then allowed to stand for 5 min at room temperature. This sample solution was diluted up to 2.5 mL with water and used for the spectroscopic measurement. The absorbance at $\lambda = 434$ nm (A_S) due to $[Ti^{IV}O(tpypH_4)]^{4+}$ was measured using a Hewlett Packard 8453 diode array spectrophotometer. In a similar manner, a blank solution was prepared by adding distilled water instead of the sample solution in the same volume with its absorbance designated as A_B. The difference in absorbance at 434 nm was determined as follows: $\Delta A_{434} = A_B - A_S$. Based on ΔA_{434} and the volume of the solution, the amount of hydrogen peroxide was determined according to the literature.[23] A Clark-type oxygen electrode was used to obtain oxygen evolution data, and calibrated daily using Ar deoxygenated and oxygen saturated atmospheric solutions. Clark electrode experiments were performed by adding 10 µL of $[Ru^{III}(Me_2phen)_3]^{3+}$ (100 mM) to an O_2-saturated solvent mixture (1.0 mL) of MeCN and H_2O (v/v = 9 : 1) containing **1** (10–200 µM) and monitoring the O_2 evolved.

Conflicts of interest

There are no conflicts to declare.

Acknowledgements

Notes and references

1 M. Weber, M. Weber and M. Kleine-Boymann, *Phenol. Ullmann's Encyclopedia of Industrial Chemistry*, Wiley-VCH Verlag GmbH & Co. KGaA, Weinheim, Germany, 2004, vol. 26, p. 503.

2 (a) R. Molinari and T. Poerio, *Asia–Pac. J. Chem. Eng.*, 2010, **5**, 191; (b) R. J. Schmidt, *Appl. Catal., A*, 2005, **280**, 89.

3 (a) L. Balducci, D. Bianchi, R. Bortolo, R. D'Aloisio, M. Ricci, R. Tassinari and R. Ungarelli, *Angew. Chem., Int. Ed.*, 2003, **42**, 4937; (b) J.-H. Yang, G. Sun, Y. Gao, H. Zhao, P. Tang, J. Tan, A.-H. Lu and D. Ma, *Energy Environ. Sci.*, 2013, **6**, 793.

4 S. Fukuzumi and K. Ohkubo, *Asian J. Org. Chem.*, 2015, **4**, 836.

5 (a) X. Cai, Q. Wang, Y. Liu, J. Xie, Z. Long, Y. Zhou and J. Wang, *ACS Sustainable Chem. Eng.*, 2016, **4**, 4986; (b) W. Wang, L. Shi, N. Li and Y. Ma, *RSC Adv.*, 2017, **7**, 12738.

6 (a) Y. Morimoto, S. Bunno, N. Fujieda, H. Sugimoto and S. Itoh, *J. Am. Chem. Soc.*, 2015, **137**, 5867; (b) Y. Aratani, Y. Yamada and S. Fukuzumi, *Chem. Commun.*, 2015, **51**, 4662.

7 (a) D. Wang, M. Wang and Z. Li, *ACS Catal.*, 2015, **5**, 6852; (b) X. Ye, Y. Cui, X. Qiu and X. Wang, *Appl. Catal., B*, 2014, **152–153**, 383; (c) G. Wen, S. Wu, B. Li, C. Dai and D. S. Su, *Angew. Chem., Int. Ed.*, 2015, **54**, 4105.

8 (a) M. Yamada, K. D. Karlin and S. Fukuzumi, *Chem. Sci.*, 2016, **7**, 2856; (b) B. Xu, W. Zhong, Z. Wei, H. Wang, J. Liu, L. Wu, Y. Feng and X. Liu, *Dalton Trans.*, 2014, **43**, 15337; (c) L. Wu, W. Zhong, B. Xu, Z. Wei and X. Liu, *Dalton Trans.*, 2015, **44**, 8013.

9 (a) W. Ge, Z. Long, X. Cai, Q. Wang, Y. Zhou, Y. Xu and J. Wang, *RSC Adv.*, 2014, **4**, 45816; (b) C. Wang, L. Hu, Y. Hu, Y. Ren, X. Chen, B. Yue and H. He, *Catal. Commun.*, 2015, **68**, 1.

10 (a) P. Borah, X. Ma, K. T. Nguyen and Y. Zhao, *Angew. Chem., Int. Ed.*, 2012, **51**, 7756; (b) P. K. Khatri, B. Singh, S. L. Jain, B. Sain and A. K. Sinha, *Chem. Commun.*, 2011, **47**, 1610; (c) Y. Leng, J. Liu, P. Jiang and J. Wang, *Chem. Eng. J.*, 2014, **239**, 1.

11 (a) H. Wang, M. Zhao, Q. Zhao, Y. Yang, C. Wang and Y. Wang, *Ind. Eng. Chem. Res.*, 2017, **56**, 2711; (b) S. Verma, R. B. N. Baig, M. N. Nadagouda and R. S. Varma, *ACS Sustainable Chem. Eng.*, 2017, **5**, 3637.

12 (a) L. Muniandy, F. Adama, A. R. Mohamed, A. Iqbal and N. R. A. Rahman, *Appl. Surf. Sci.*, 2017, **398**, 43; (b) J. Xu, Q. Jiang, T. Chen, F. Wu and Y.-X. Li, *Catal. Sci. Technol.*, 2015, **5**, 1504; (c) P. R. Makgwane and S. S. Raya, *J. Mol. Catal. A: Chem.*, 2015, **398**, 149.

13 (a) L. Carneiro and A. R. Silva, *Catal. Sci. Technol.*, 2016, **6**, 8166; (b) E. Gu, W. Zhong and X. Liu, *RSC Adv.*, 2016, **6**, 98406; (c) E. Gu, W. Zhong, H. Ma, B. Xu, H. Wang and X. Liu, *Inorg. Chim. Acta*, 2016, **444**, 159; (d) B. Xu, W. Zhong, Z. Wei, H. Wang, J. Liu, L. Wu, Y. Feng and X. Liu, *Dalton Trans.*, 2014, **43**, 15337.

14 (a) S. Niwa, M. Eswaramoorthy, J. Nair, A. Raj, N. Itoh, H. Shoji, T. Namba and F. Mizukami, *Science*, 2002, **295**,

105; (b) K. Sato, T. Hanaoka, S. Niwa, C. Stefan, T. Namba and F. Mizukami, *Catal. Today*, 2005, **104**, 260.

15 (a) A. Okemoto, Y. Tsukano, A. Utsunomiya, K. Taniya, Y. Ichihashi and S. Nishiyama, *J. Mol. Catal. A: Chem.*, 2016, **411**, 372; (b) B. B. Sarma, R. Carmieli, A. Collauto, I. Efremenko, J. M. L. Martin and R. Neumann, *ACS Catal.*, 2016, **6**, 6403.

16 (a) Z. Long, Y. Zhou, W. Ge, G. Chen, J. Xie, Q. Wang and J. Wang, *ChemPlusChem*, 2014, **79**, 1590; (b) Z. Long, Y. Zhou, G. Chen, P. Zhao and J. Wang, *Chem. Eng. J.*, 2014, **239**, 19; (c) S. Shang, B. Chen, L. Wang, W. Dai, Y. Zhang and S. Gao, *RSC Adv.*, 2015, **5**, 31965.

17 Y. Aratani, K. Oyama, T. Suenobu, Y. Yamada and S. Fukuzumi, *Inorg. Chem.*, 2016, **55**, 5780.

18 (a) R. Hamada, Y. Shibata, S. Nishiyama and S. Tsuruya, *Phys. Chem. Chem. Phys.*, 2003, **5**, 956; (b) Z. Long, Y. Zhou, G. Chen, W. Ge and J. Wang, *Sci. Rep.*, 2014, **4**, 3651; (c) Z. Long, Y. Liu, P. Zhao, Q. Wang, Y. Zhou and J. Wang, *Catal. Commun.*, 2015, **59**, 1; (d) S. S. Acharyya, S. Ghosh, R. Tiwari, C. Pendem, T. Sasaki and R. Bal, *ACS Catal.*, 2015, **5**, 2850; (e) R. Bal, M. Tada, T. Sasaki and Y. Iwasawa, *Angew. Chem., Int. Ed.*, 2006, **45**, 448.

19 (a) T. D. Bui, A. Kimura, S. Ikeda and M. Matsumura, *J. Am. Chem. Soc.*, 2010, **132**, 8453; (b) Y. Ide, M. Torii and T. Sano, *J. Am. Chem. Soc.*, 2013, **135**, 11784; (c) Y. Ide, M. Matsuoka and M. Ogawa, *J. Am. Chem. Soc.*, 2010, **132**, 16762.

20 K. Ohkubo, T. Kobayashi and S. Fukuzumi, *Angew. Chem., Int. Ed.*, 2011, **50**, 8652.

21 K. Ohkubo, A. Fujimoto and S. Fukuzumi, *J. Am. Chem. Soc.*, 2013, **135**, 5368.

22 K. Ohkubo, K. Hirose and S. Fukuzumi, *Chem.–Eur. J.*, 2015, **21**, 2855.

23 S. Kato, J. Jung, T. Suenobu and S. Fukuzumi, *Energy Environ. Sci.*, 2013, **6**, 3756.

24 (a) Y. Isaka, S. Kato, D. Hong, T. Suenobu, Y. Yamada and S. Fukuzumi, *J. Mater. Chem. A*, 2015, **3**, 12404; (b) Y. Isaka, K. Oyama, Y. Yamada, T. Suenobu and S. Fukuzumi, *Catal. Sci. Technol.*, 2016, **6**, 681.

25 (a) A. Das, V. Joshi, D. Kotkar, V. S. Pathak, V. Swayambunathan, P. V. Kamat and P. K. Ghosh, *J. Phys. Chem. A*, 2001, **105**, 6945; (b) D. Hong, J. Jung, J. Park, Y. Yamada, T. Suenobu, Y.-M. Lee, W. Nam and S. Fukuzumi, *Energy Environ. Sci.*, 2012, **5**, 7606.

26 It should be noted, however, that the contribution from the catalytic hydroxylation of benzene with $[Ru^{III}(bpy)_3]^{3+}$ in competition with H_2O oxidation cannot be ruled out.

27 (a) S. Fukuzumi and K. Ohkubo, *Chem.–Eur. J.*, 2000, **6**, 4532; (b) S. Fukuzumi, M. Patz, T. Suenobu, Y. Kuwahara and S. Itoh, *J. Am. Chem. Soc.*, 1999, **121**, 1605; (c) S. Fukuzumi, H. Ohtsu, K. Ohkubo, S. Itoh and H. Imahori, *Coord. Chem. Rev.*, 2002, **226**, 71.

28 W. L. F. Armarego and C. L. L. Chai, in *Purification of Laboratory Chemicals*, Pergamon Press, Oxford, U. K., 6th edn, 2009.

29 (a) S. Hong, F. F. Pfaff, E. Kwon, Y. Wang, M.-S. Seo, E. Bill, K. Ray and W. Nam, *Angew. Chem., Int. Ed*, 2014, **53**, 10403; (b) B. Wang, Y.-M. Lee, W.-Y. Tcho, S. Tussupbayev, S.-T. Kim, Y. Kim, M. S. Seo, K.-B. Cho, Y. Dede, B. C. Keegan, T. Ogura, S. H. Kim, T. Ohta, M.-H. Baik, K. Ray, J. Shearer and W. Nam, *Nat. Commun.*, 2016, **8**, 14839.

30 C. Turro, J. M. Zaleski, Y. M. Karabatsos and D. G. Nocera, *J. Am. Chem. Soc.*, 1996, **118**, 6060.

31 C. Matsubara, N. Kawamoto and K. Takamura, *Analyst*, 1992, **117**, 1781.